

**$\alpha$ -decay branching ratio of  $^{180}\text{Pt}$** 

J. G. Cubiss<sup>1,\*</sup> R. D. Harding,<sup>1,2</sup> A. N. Andreyev,<sup>1,3</sup> N. Althubiti,<sup>4,5</sup> B. Andel<sup>6,7</sup> S. Antalic<sup>6</sup> A. E. Barzakh,<sup>8</sup> T. E. Cocolios<sup>7,4</sup> T. Day Goodacre,<sup>4,2,†</sup> G. J. Farooq-Smith,<sup>4,7</sup> D. V. Fedorov,<sup>8</sup> V. N. Fedosseev<sup>6,2</sup> L. P. Gaffney<sup>9,7,‡</sup> L. Ghys,<sup>10,7</sup> M. Huyse,<sup>7</sup> K. M. Lynch,<sup>2</sup> B. A. Marsh,<sup>2</sup> Y. Martinez Palenzuela,<sup>7</sup> P. L. Molkanov,<sup>8</sup> R. E. Rossel,<sup>2,11</sup> S. Rothe,<sup>2</sup> M. D. Seliverstov<sup>6,8</sup> S. Sels<sup>6,7,§</sup> P. Spagnoletti<sup>6,9</sup> C. Van Beveren,<sup>7</sup> P. Van Duppen<sup>6,7</sup> M. Veinhard,<sup>2</sup> E. Verstraelen,<sup>7</sup> and A. Zadvornaya<sup>7,||</sup>

<sup>1</sup>Department of Physics, University of York, York YO10 5DD, United Kingdom

<sup>2</sup>CERN, CH-1211 Geneva 23, Switzerland

<sup>3</sup>Advanced Science Research Center (ASRC), Japan Atomic Energy Agency (JAEA), Tokai-mura, Ibaraki 319-1195, Japan

<sup>4</sup>School of Physics and Astronomy, The University of Manchester, Manchester M13 9PL, United Kingdom

<sup>5</sup>Physics Department, Faculty of Science, Jouf University, Aljouf, Saudi Arabia

<sup>6</sup>Department of Nuclear Physics and Biophysics, Comenius University in Bratislava, 84248 Bratislava, Slovakia

<sup>7</sup>KU Leuven, Instituut voor Kern- en Stralingsfysica, B-3001 Leuven, Belgium

<sup>8</sup>Petersburg Nuclear Physics Institute, NRC Kurchatov Institute, Gatchina 188300, Russia

<sup>9</sup>School of Engineering and Computing, University of the West of Scotland, Paisley PA1 2BE, United Kingdom

<sup>10</sup>Belgian Nuclear Research Center SCK•CEN, Boeretang 200, B-2400 Mol, Belgium

<sup>11</sup>Institut für Physik, Johannes Gutenberg-Universität, 55122 Mainz, Germany



(Received 6 October 2019; published 21 January 2020)

A study of the  $^{180}\text{Hg}$  decay chain performed at the CERN-ISOLDE facility has allowed the ground-state-to-ground-state  $\alpha$  decay of  $^{180}\text{Pt}$  to be investigated. A more precise  $\alpha$ -decay branching ratio of  $b_\alpha(^{180}\text{Pt}) = 0.52(5)\%$  has been deduced. The reduced  $\alpha$ -decay width calculated using the new value provides a more consistent picture of the systematics for  $J^\pi = 0^+ \rightarrow 0^+$  ground-state-to-ground-state state  $\alpha$  decays of neutron-deficient, even-even platinum isotopes.

DOI: [10.1103/PhysRevC.101.014314](https://doi.org/10.1103/PhysRevC.101.014314)

## I. INTRODUCTION

Alpha decay is a useful probe for studying the underlying structures of nuclei involved in the process. For example, reduced  $\alpha$ -decay widths ( $\delta_\alpha^2$ ) are particularly sensitive to the overlap in wave function between the initial and final states connected by the decay [1]. These may be calculated, for instance, using the Rasmussen approach [2], which requires experimental  $\alpha$ -decay energies and partial half-lives. The latter are dependent on  $\alpha$ -decay branching ratios ( $b_\alpha$ ), which are often challenging to measure in nuclei with small  $b_\alpha$  values

due to only low statistics and/or the presence of more intense  $\alpha$  decays.

In this work, we report on a more precise  $b_\alpha$  for the  $^{180}\text{Pt}$  ground state (g.s.). This value was extracted from decay data recorded during the same experiment as described in Refs. [3,4].

The currently accepted value  $b_\alpha(^{180}\text{Pt}) \approx 0.3\%$  came from a study by Siivola [5], in which  $^{180}\text{Pt}$  was produced in  $^{16}\text{O} + ^{170,172}\text{Yb}$ ,  $^{19}\text{F} + ^{169}\text{Tm}$ , and  $^{20}\text{Ne} + ^{162}\text{Er}$  fusion-evaporation reactions. The  $b_\alpha$  values for several platinum isotopes were deduced by comparing measured  $\alpha$ -decay intensities to expected production yields, based on similar heavy-ion reactions studied in the rare-earth region. Due to this approach, the extracted value of  $b_\alpha(^{180}\text{Pt}) \approx 0.3\%$  had a large uncertainty factor of 3–5 [5].

## II. EXPERIMENT

A detailed description of the experiment can be found in Refs. [3,4], while only the information pertinent to the present work is provided here. In our study,  $^{180}\text{Pt}$  was produced in the  $^{180}\text{Hg} \rightarrow ^{180}\text{Au} \rightarrow ^{180}\text{Pt}$   $\beta$ -decay chain, shown in Fig. 1. An isotopically pure ion beam of  $^{180}\text{Hg}$  was produced at the ISOLDE facility [13,14] through spallation reactions induced by a 1.4-GeV proton beam impinging upon a molten lead target, followed by a three-step, resonance laser ionization

\*james.cubiss@york.ac.uk

<sup>†</sup>Present address: TRIUMF, 4004 Wesbrook Mall, Vancouver, BC, Canada V6T 2A3.

<sup>‡</sup>Present address: Oliver Lodge Laboratory, University of Liverpool, Liverpool L69 7ZE, United Kingdom.

<sup>§</sup>Present address: CERN, CH-1211 Geneva 23, Switzerland.

<sup>||</sup>Present address: Department of Physics, University of Jyväskylä, P.O. Box 35, SF-40351, Finland.

Published by the American Physical Society under the terms of the [Creative Commons Attribution 4.0 International](https://creativecommons.org/licenses/by/4.0/) license. Further distribution of this work must maintain attribution to the author(s) and the published article's title, journal citation, and DOI.

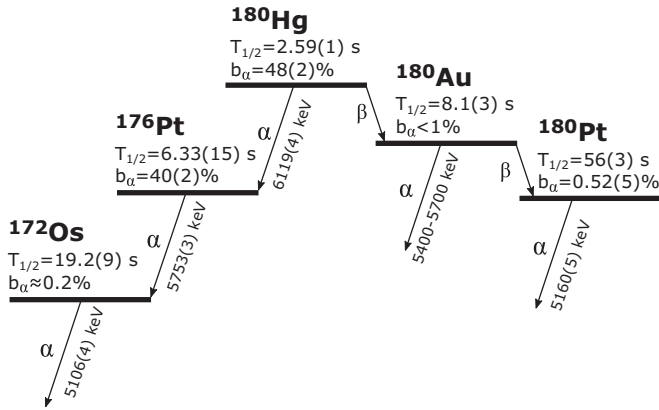


FIG. 1. Schematic of the  $^{180}\text{Hg}$  decay chain, showing the isotopes and  $\alpha$ -decay energies important to the present work. The  $b_{\alpha}(^{180}\text{Pt}) = 0.52(5)\%$  value is taken from the results of our study (see Sec. III), and  $E_{\alpha}(^{180}\text{Pt}) = 5160(5)$  keV is from Ref. [6]. All other data are taken from Refs. [7–12].

process in the VADLIS [15,16] in order to selectively ionize the mercury atoms of interest. The ions were extracted and accelerated by a 30-kV potential difference, and separated according to their mass-to-charge ratio by the ISOLDE general purpose separator.

The  $^{180}\text{Hg}$  ion beam was then delivered to the Windmill system [17,18] for decay measurements. The beam entered the Windmill through the central hole of an annular silicon detector (Si1), and was implanted into one of ten,  $20\text{-}\mu\text{g cm}^{-2}$ -thick carbon foils mounted upon a rotatable wheel. A second silicon detector (Si2) was placed a few millimeters behind the foil being irradiated. The data presented in the current work were taken in runs where the wheel was not rotated to avoid loss of activity during the dedicated  $b_{\alpha}$  measurements. Furthermore, due to the specific conditions during this measurement, only events recorded in Si2 were used in the following analysis. The full width at half maxima of the  $\alpha$ -decay peaks recorded by Si2 within the  $E_{\alpha} = 5000\text{--}6200$ -keV region of interest were  $\approx 30$  keV.

The energy calibration for Si2 was performed using  $E_{\alpha}(^{180}\text{Hg}) = 6119(4)$  keV [19] and  $E_{\alpha}(^{180}\text{Pt}) = 5160(5)$  keV for the g.s.-to-g.s. decay of  $^{180}\text{Pt}$ . The latter was deduced in our recent study of gold isotopes and will be discussed in Ref. [6]. Our new value differs significantly from  $E_{\alpha}(^{180}\text{Pt}) = 5140(10)$  keV reported by Siivola [5] but has a higher precision. In addition to the energy calibration, our  $E_{\alpha}(^{180}\text{Pt})$  value will be used in the  $\delta_{\alpha}^2$  calculations presented in Sec. IV.

### III. RESULTS

Figure 2(a) shows the singles  $\alpha$ -decay spectrum recorded by Si2. The spectrum readily illustrates the purity of the  $^{180}\text{Hg}$  beam, as only the decays of  $^{180}\text{Hg}$ , its daughter and its granddaughter nuclei are seen.

The two most intense peaks in Fig. 2(a) belong to the well-known decays of  $^{180}\text{Hg}$  [ $E_{\alpha} = 6119(4)$  keV] [19] and  $^{176}\text{Pt}$  [ $E_{\alpha} = 5753(3)$  keV] [8]. The low-intensity  $E_{\alpha}(^{180}\text{Hg}) = 5862(5)$  keV fine-structure (f.s.) decay is also visible [20]. The

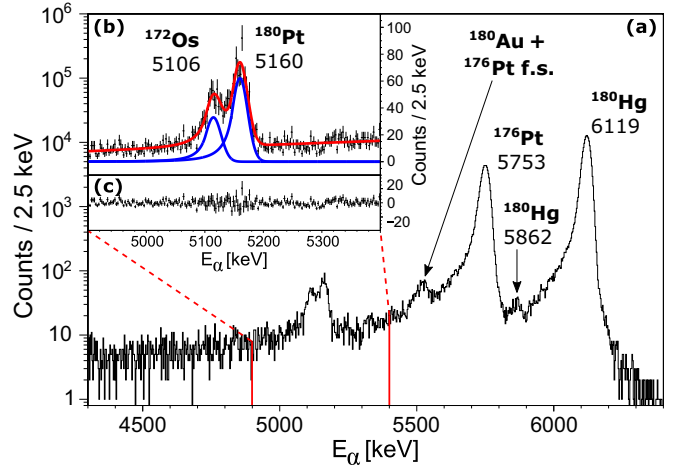


FIG. 2. (a) Energy spectrum of singles  $\alpha$ -decay events measured in Si2 at  $A = 180$ , (b) zoomed view of the 4900–5400-keV region, fitted with a linear background plus two Crystal Ball functions (red line), the individual contributions from the  $\alpha$  decays of  $^{172}\text{Os}$  and  $^{180}\text{Pt}$  are shown by the blue lines, (c) the residual between the fit and the data shown in panel (b). The main  $\alpha$ -decay peaks are labeled with the corresponding isotope and  $\alpha$ -particle energies.

structure seen in the  $E_{\alpha} = 5460\text{--}5560$ -keV region is due to the f.s.  $\alpha$  line of  $^{176}\text{Pt}$  [ $E_{\alpha} = 5530(3)$  keV] [12] and the complex f.s. decay of  $^{180}\text{Au}$  [6,20,21]. The  $\alpha$ -decay peak of  $^{180}\text{Pt}$  is seen to be partially overlapping with the 5106(4)-keV  $^{172}\text{Os}$   $\alpha$ -decay peak [12]. The two peaks lie on top of a significant background from the low-energy tails of the higher-energy and higher-intensity  $\alpha$  decays of  $^{176}\text{Pt}$  and  $^{180}\text{Hg}$ .

The g.s.-to-g.s.  $b_{\alpha}(^{180}\text{Pt})$  value was deduced by using the number of  $^{180}\text{Hg}$   $\alpha$  decays in Fig. 2,  $N_{\alpha}(^{180}\text{Hg})$ , to calculate the number of  $\beta$  decays feeding to  $^{180}\text{Au}$  and then to  $^{180}\text{Pt}$  (see decay scheme in Fig. 1). This approach treats the number of  $^{180}\text{Au}$  and  $^{180}\text{Hg}$   $\beta$  decays as approximately equal, as the correction for the small  $^{180}\text{Au}$   $\alpha$ -decay branch [ $b_{\alpha}(^{180}\text{Au}) \approx 0.6\%$  taken from Ref. [6]]<sup>1</sup> is negligible compared to the statistical error on  $N_{\alpha}(^{180}\text{Pt})$  extracted from Fig. 2 ( $\approx 10\%$ ). Thus,  $N_{\alpha}(^{180}\text{Hg})$  and  $N_{\alpha}(^{180}\text{Pt})$  may be directly compared in order to calculate  $b_{\alpha}(^{180}\text{Pt})$ , such that

$$b_{\alpha}(^{180}\text{Pt}) = \frac{N_{\alpha}(^{180}\text{Pt})}{\frac{N_{\alpha}(^{180}\text{Hg})}{b_{\alpha}(^{180}\text{Hg})} (1 - b_{\alpha}(^{180}\text{Hg}))}, \quad (1)$$

where  $b_{\alpha}(^{180}\text{Hg}) = 48(2)\%$  [11,12].

To evaluate  $N_{\alpha}(^{180}\text{Pt})$ , the  $E_{\alpha} = 4900\text{--}5900$ -keV region of Fig. 2(b) was fitted with the ROOT Minuit minimizer [22], using a binned-likelihood method. A linear function was used to model the background and Crystal Ball functions [23–25], which shared the same set of parameters to describe the width and tails of the peaks were used for the  $^{180}\text{Pt}$  and

<sup>1</sup>A study at SHIP [21] deduced a lower limit of  $b_{\alpha}(^{180}\text{Au}) > 1.8\%$ . However, this limit was calculated using the  $b_{\alpha}(^{180}\text{Pt}) \approx 0.3\%$  value with the factor of 3–5 uncertainty [5]. Furthermore, the expression used to calculate  $b_{\alpha}(^{180}\text{Au})$  was incorrect (see Table 2 in Ref. [21]), as confirmed in private communications with the authors of the study.

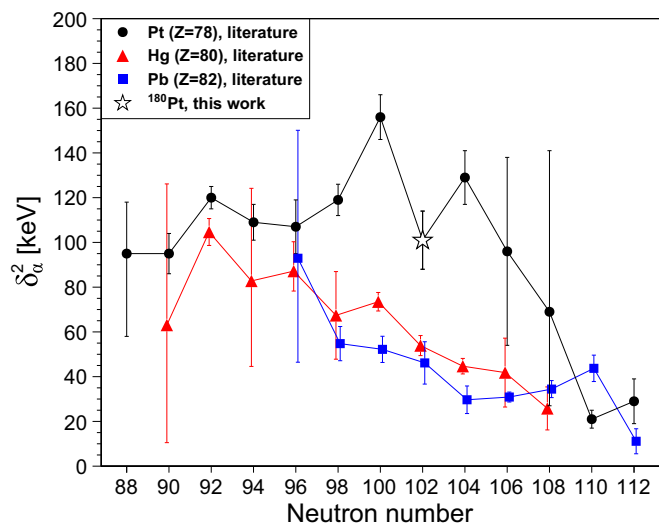


FIG. 3. Reduced  $\alpha$ -decay widths for  $J^\pi = 0^+ \rightarrow 0^+$ , g.s.-to-g.s. decays of even- $A$  platinum ( $\bullet$ ), mercury ( $\blacktriangle$ ), and lead ( $\blacksquare$ ) isotopes, calculated using the Rasmussen approach [2] with data taken from Refs. [8–12,26,27]. The open star is the  $\delta_\alpha^2(^{180}\text{Pt})$  calculated using the results from the present work and Ref. [6].

$^{172}\text{Os}$   $\alpha$ -decay peaks. The red line in Fig. 2(b) shows the result of the fitting procedure, the blue lines represent the contributions from the  $^{180}\text{Pt}$  and  $^{172}\text{Os}$   $\alpha$  decays. Figure 2(c) shows the residual between the result of the fitting procedure and the data shown in Fig. 2(b). The  $N_\alpha(^{180}\text{Hg})$  value was assessed in a similar way, however we assumed background-free conditions. Using the results from the fitting procedure a value of  $b_\alpha(^{180}\text{Pt}) = 0.52(5)\%$  was deduced.

#### IV. DISCUSSION

The reduced widths of  $J^\pi = 0^+ \rightarrow 0^+$  g.s.-to-g.s. decays of even- $A$  platinum isotopes calculated using the Rasmussen approach [2] are shown in Fig. 3, along with those for even- $A$  mercury and lead isotopes. The open star represents  $\delta_\alpha^2(^{180}\text{Pt}) = 101(13)$  keV, calculated using the  $b_\alpha$  value from the current work and  $E_\alpha = 5160(5)$  keV from Ref. [6].

In general, Fig. 3 displays the expected behavior (see Fig. 3 in Ref. [28] and Fig. 4 in Ref. [29]), whereby the  $\delta_\alpha^2(0^+_{\text{g.s.}} \rightarrow 0^+_{\text{g.s.}})$  values, or equivalently the  $\alpha$ -particle preformation probabilities, decrease as the proton number approaches  $Z = 82$ . This trend was interpreted in Ref. [28] as an effect of the  $Z = 82$  shell closure on the  $\alpha$ -decay process. As further shown in Ref. [29], the  $N = 126$  shell closure displays a similar influence, whereby  $\delta_\alpha^2$  values at  $N = 126$  are the smallest along an isotopic chain and an increase followed by a saturation in  $\delta_\alpha^2$  is observed as  $N$  reduces towards and beyond the  $N = 104$  midshell.

Our new  $\delta_\alpha^2(^{180}\text{Pt})$  value is first of all in better agreement with these systematics than  $\delta_\alpha^2(^{180}\text{Pt}) = 74$  keV calculated using the data from Ref. [5]. Furthermore, the new value

reveals that as expected [29] the  $\delta_\alpha^2$  for platinum isotopes is saturated in the  $88 \leq N \leq 104$  region, with near-constant values of  $\delta_\alpha^2 \approx 113$  keV.

One noticeable feature in Fig. 3 is the  $\delta_\alpha^2 = 156(10)$ -keV value for  $^{178}\text{Pt}$  ( $N = 100$ ) which is  $\approx 30\%$  larger than those of other platinum isotopes in the saturation region. The  $T_{1/2}(^{178}\text{Pt})$  [30–32] and  $b_\alpha(^{178}\text{Pt})$  [33,34] values from different studies are consistent with one another, which suggests that the experimental  $\delta_\alpha^2(^{178}\text{Pt})$  value is reliable. Therefore the jump in  $\delta_\alpha^2$  could possibly be related to the change in deformation when going from  $^{178}\text{Pt}$  to  $^{180}\text{Pt}$  [35], and related to the possible change in the configuration mixing in the corresponding ground states [20,36,37]. Alternatively, this could be a sign of evolving nuclear structures between the  $\alpha$ -decay daughter nuclei,  $^{174,176}\text{Os}$ .

In addition to the large  $\delta_\alpha^2(^{178}\text{Pt})$  value, the other noticeable features of the platinum chain in Fig. 3 are the sizable error bars on  $\delta_\alpha^2(^{184,186}\text{Pt})$  ( $N = 106, 108$ ). More precise measurements of  $b_\alpha(^{184,186}\text{Pt})$  are required in order to determine whether there is a smooth transition towards the saturated  $\delta_\alpha^2$  values, as would usually be expected.

#### V. CONCLUSION

Decay data recorded at the CERN-ISOLDE facility have been used to deduce a more precise value of  $b_\alpha(^{180}\text{Pt}) = 0.52(5)\%$ . This value has been used to calculate the reduced width of the  $^{180}\text{Pt}$  g.s.-to-g.s.  $\alpha$  decay, which is in better agreement with the  $\delta_\alpha^2$  systematics in the region than the value calculated using the current literature value.

#### ACKNOWLEDGMENTS

We would like to thank the ISOLDE collaboration and technical staff for providing excellent assistance during the experiment. This project has received funding from the European Union’s Horizon 2020 research and innovation program and the Seventh Framework Programme for Research and Technological Development under Grant Agreements No. 262010 (ENSAR), No. 654002 (ENSAR2), No. 267194 (CO-FUND), No. 289191 (LA<sup>3</sup>NET), and No. 654002 (ERC-2011-AdG-291561-HELIOS). This work was supported by RFBR according to Research Project No. 19-02-00005, by the Slovak Grant Agency VEGA (Contract No. 1/0532/17), Slovak Research and Development Agency (Contract No. APVV-14-0524), by FWO-Vlaanderen (Belgium), by GOA/2010/010 (BOF KU Leuven), and by the IAP Belgian Science Policy (BriX network P7/12). This project was partially funded by a grant from the UK Science and Technology Facilities Council (STFC): Consolidated Grant No. ST/L005794/1. S.S. acknowledges a SB Ph.D. grant from the former Belgian Agency for Innovation by Science and Technology (IWT), now incorporated in FWO-Vlaanderen. L.P.G. acknowledges FWO-Vlaanderen (Belgium) as an FWO Pegasus Marie Curie Fellow.

- [1] P. Van Duppen and M. Huyse, *Hyperfine Interact.* **129**, 149 (2000).
- [2] J. O. Rasmussen, *Phys. Rev.* **113**, 1593 (1959).
- [3] B. A. Marsh *et al.*, *Nat. Phys.* **14**, 1163 (2018).
- [4] S. Sels *et al.*, *Phys. Rev. C* **99**, 044306 (2019).
- [5] A. Siivola, *Nucl. Phys.* **84**, 385 (1966).
- [6] R. D. Harding *et al.* (unpublished).
- [7] J. Husson, C. Liang, and C. Richard-Serre, *J. Physique Lett.* **38**, 245 (1977).
- [8] B. Singh, *Nucl. Data Sheets* **75**, 199 (1995).
- [9] M. Basunia, *Nucl. Data Sheets* **107**, 791 (2006).
- [10] C. M. Baglin, *Nucl. Data Sheets* **111**, 1807 (2010).
- [11] E. McCutchan, *Nucl. Data Sheets* **126**, 151 (2015).
- [12] NNDC, Evaluated Nuclear Structure Data File, 2019.
- [13] E. Kugler, *Hyperfine Interact.* **129**, 23 (2000).
- [14] R. Catherall, W. Andreatza, M. Breitenfeldt, A. Dorsival, G. J. Focker, T. P. Gharsa, T. J. Giles, J.-L. Grenard, F. Locci, P. Martins *et al.*, *J. Phys. G: Nucl. Part. Phys.* **44**, 094002 (2017).
- [15] T. Day Goodacre *et al.*, *Nucl. Instrum. Methods Phys. Res., Sect. B* **376**, 39 (2016).
- [16] Y. Martinez Palenzuela *et al.*, *Nucl. Instrum. Methods Phys. Res., Sect. B* **431**, 59 (2018).
- [17] J. G. Cubiss *et al.*, *Phys. Rev. C* **97**, 054327 (2018).
- [18] A. N. Andreyev *et al.*, *Phys. Rev. Lett.* **105**, 252502 (2010).
- [19] F. G. Kondev *et al.*, *Phys. Rev. C* **62**, 044305 (2000).
- [20] J. Wauters, P. Dendooven, M. Huyse, G. Reusen, P. Van Duppen, R. Kirchner, O. Klepper, and E. Roeckl, *Z. Phys. A: Hadrons Nucl.* **345**, 21 (1993).
- [21] J. G. Keller, K.-H. Schmidt, F. P. Hessberger, G. Münzenberg, W. Reisdorf, H.-G. Clerc, and C.-C. Sahn, *Nucl. Phys. A* **452**, 173 (1986).
- [22] F. James and M. Roos, *Comput. Phys. Commun.* **10**, 343 (1975).
- [23] M. J. Oreglia, Ph.D. thesis, SLAC-R-236, 1980.
- [24] J. E. Gaiser, Ph.D. thesis, SLAC-R-255, 1982.
- [25] T. Skwarnicki, Ph.D. thesis, DESY F31-86-02, 1986.
- [26] H. Badran *et al.*, *Phys. Rev. C* **94**, 054301 (2016).
- [27] J. Hilton *et al.*, *Phys. Rev. C* **100**, 014305 (2019).
- [28] A. N. Andreyev *et al.*, *Phys. Rev. Lett.* **110**, 242502 (2013).
- [29] C. Qi, A. N. Andreyev, M. Huyse, R. J. Liotta, P. Van Duppen, and R. Wyss, *Phys. Lett. B* **734**, 203 (2014).
- [30] J. D. Bowman, R. E. Eppley, and E. K. Hyde, *Phys. Rev. C* **25**, 941 (1982).
- [31] F. Meissner, H. Salewski, W. D. Schmidt-Ott, U. Bosch-Wicke, V. Kunze, and R. Michaelsen, *Phys. Rev. C* **48**, 2089 (1993).
- [32] F. G. Kondev *et al.*, *Phys. Rev. C* **61**, 044323 (2000).
- [33] P. G. Hansen, H. L. Nielsen, K. Wilsky, M. Alpsten, M. Finger, A. Lindahl, R. A. Naumann, and O. B. Nielsen, *Nucl. Phys. A* **148**, 249 (1970).
- [34] U. J. Schrewe *et al.*, *Phys. Lett. B* **91**, 46 (1980).
- [35] F. Le Blanc *et al.*, *Phys. Rev. C* **60**, 054310 (1999).
- [36] G. D. Dracoulis, B. Fabricius, A. E. Stuchbery, A. O. Macchiavelli, W. Korten, F. Azaiez, E. Rubel, M. A. Deleplanque, R. M. Diamond, and F. S. Stephens, *Phys. Rev. C* **44**, R1246 (1991).
- [37] J. L. Wood, K. Heyde, W. Nazarewicz, M. Huyse, and P. van Duppen, *Phys. Rep.* **215**, 101 (1992).